ICANS-XV
15th Meeting of the International Collaboration on Advanced Neutron Sources
November 6 – 9, 2000
Tsukuba, Japan

23.1
Overview of the ESS Target and Moderator R&D

Harald Conrad and Hans Ullmaier

ESS Project
Forschungszentrum Jülich GmbH

Abstract

The major concern in current R&D effort is radiation damage and foreign atom production (mainly hydrogen and helium) in structural materials of the ESS mercury target. Mechanical tests on specimens from spent targets at LAMPF and ISIS are being performed. The results show a remarkable strengthening and embrittlement with all three investigated materials classes (austenitic and martensitic steels as well as nickel-based alloys). The residual ductility observed with specimens subject to the highest available dose of 10 dpa (corresponding to about 2 months of operation of ESS) are, however, sufficient for being employed as structural materials of ESS targets. Furthermore, an additional extended irradiation program at PSI (STIP) is just about to be started.

Pressure waves in mercury as well as the resulting stress waves in the container walls of the ASTE mercury target are being investigated at the AGS in Brookhaven. A comparison with results from finite elements calculations is under way.

Heat transfer experiments in mercury loops in connection with computational fluid dynamics studies are being conducted. This is to investigate the active cooling of the proton beam window of the target container.

Within the present R&D phase several paths for developing radiation resistant or at least better manageable cold moderators such as small pebbles of solid methane (2 to 3 mm diameter) or methane clathrates (e.g. from water ice) are being pursued. Irradiation behavior of solid methane is being performed at the IBR-2 reactor in Russia. The neutronic properties (intensities and pulse shapes) of the different variants will be studied employing the ESS target-moderator-reflector module JESSICA, which became operational recently at the Jülich Cooler Synchrotron.

1. Introductory remarks

It is beyond the scope of this presentation to give a comprehensive view of the entire R&D work being performed concerning target and moderator issues. We have selected the so far most thoroughly investigated tasks including some remarks on recently started activities. The emphasis of this research is on the most highly loaded components, i.e. target and moderators. The integrity of these parts clearly will be decisive for the duration of uninterrupted operation periods of the entire facility. The extraordinary loads on the mercury target are on the container proper and its secondary enclosure, in particular, where the protons penetrate the respective beam windows. Of these loads, radiation damage and foreign atom production (mainly hydrogen and helium) are of particular concern. The other major concern, stress waves, will be discussed in a different section.

2. Radiation-induced Changes of Mechanical Properties of Target Structural Materials

The lifetime of the ESS target structure (proton beam window, return hull, Hg-container) will be determined by radiation damage (displacements per atom, dpa) and H- and He- production due to high energy protons and neutrons [1]. Because of the different radiation conditions, data from fission and fusion materials research cannot be directly transferred to the spallation case. At present, the only supply of information are specimens obtained from spent target components of already operating medium-power sources such as ISIS (UK) and LANSCE (USA). The ESS-target group has collected all available high dose components of these sources in the Hot Cells of the FZ-Jülich. Specimen preparation and first mechanical test were started in 1997. A detailed discussion of the present test program is presented by F. Carsughi [2]. The results obtained up to now [3-5] can be summarized as follows:

The irradiation causes a hardening/strengthening connected with a decrease in ductility (the so-called low-temperature embrittlement) in all 3 investigated types of materials, Fig. 1: an austenitic stainless steel (AISI 304 L), a martensitic/ferritic steel (DIN 1.4926) and a high-strength Ni-based alloy (Inconel 718). The fracture mode is, however, different: whereas the fracture remains transgranular for 1.4926, it changes from ductile transgranular in the initial material (see Fig. 2a) to brittle intergranular in 304 L (see Fig. 2c) and Inconel 718. At present detailed transmission-electron-microscope (TEM) investigations are under way to correlate the mechanical behaviour with the irradiation-induced changes of the microstructure.

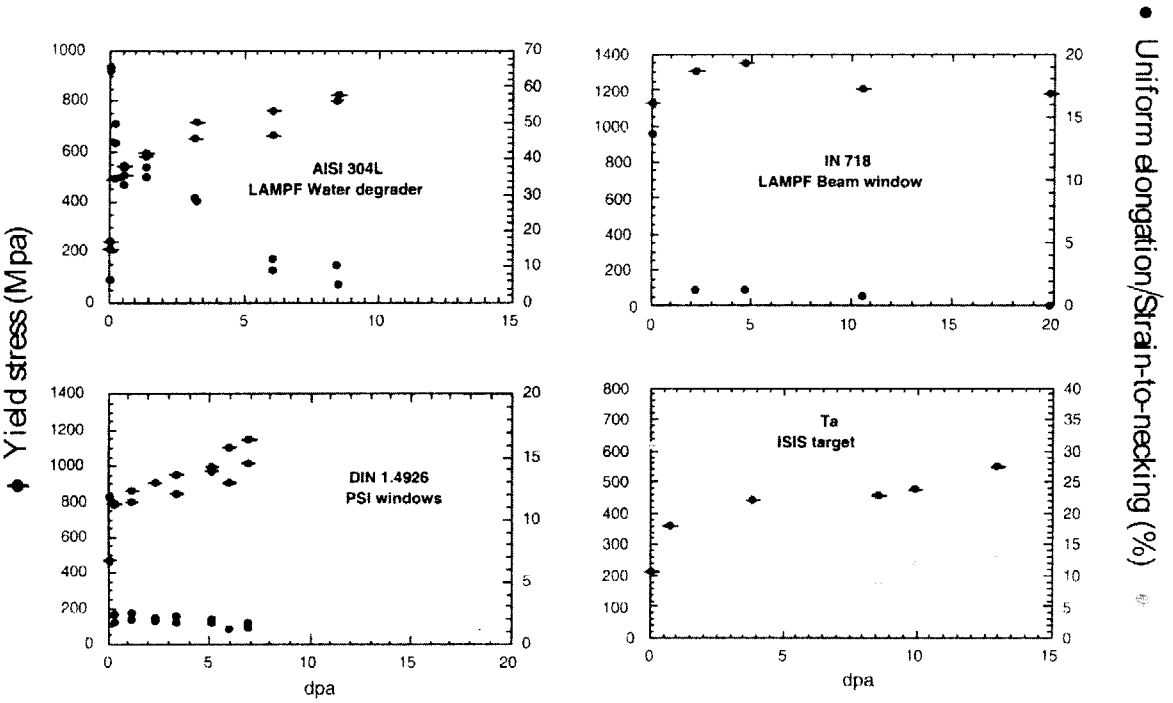

Fig.1: Yield strength, uniform elongation resp. strain to necking measured at 20°C vs. displacement dose after 800 MeV proton irradiation for austenitic steel AISI 304 L, martensitic steel DIN 1.4926, a Nickel-based alloy IN 718 and Tantalum.

The maximum doses available up to now are limited to about 10 dpa which corresponds to a full power operation time of about 2 months for ESS conditions. The observed ductilities at this dose level are small (>1%) but acceptable, especially if the fracture toughnesses of >50 $MPam^{1/2}$ measured in similar specimens is taken into account.

Higher dose levels are expected from the international irradiation programme STIP in the SINQ target. First specimens should soon arrive in Jülich for mechanical tests in the hot cells.

Complementary information, especially on the basic radiation damage mechanisms is obtained by simulation irradiations with light ions from the Jülich Kompakt-Zyklotron. A preliminary analysis of the data suggests that the observed changes of properties are mainly due to displacement effects whereas the simultaneously produced helium plays only a minor role for concentrations below several 0.1 at %.

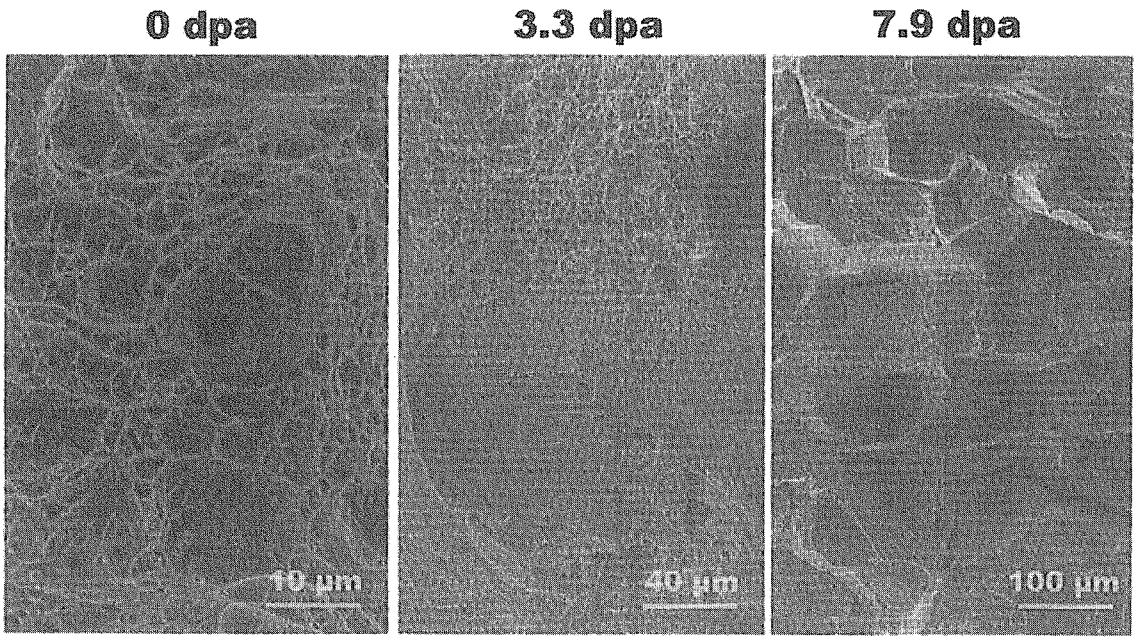

Fig. 2: Scanning electron micrographs of fracture surfaces of 304 L steel after tensile testing for unirradiated reference material and specimens after irradiation to 3.3 dpa and 7.9 dpa, respectively. The change in fracture mode from ductile-transgranular to brittle-intergranular is clearly seen.

3. The stress wave problem

Stress waves within the container walls of liquid metal targets are generated by direct heating of the beam window as well as by pressure waves due to the pulsed heating of the liquid metal. Early calculations indicated that the stresses in the container wall of a 5 MW mercury target may be already beyond admissible limits [6]. Experiments on this crucial issue have been planned and performed at the Alternating Gradient Synchrotron (AGS) in Brookhaven with the mercury target of the international ASTE (AGS Spallation Target Experiment) collaboration. Using a recently developed laser interferometric technique for measuring pressure waves in liquid metal targets provided reproducible results.

On the other hand, the comparison of the ASTE experimental results with finite elements calculations (ABAQUS) of the pressure waves within the ASTE target turned out to be satisfactory only for the time interval between power input and arrival of the pressure wave front at the target container wall after about 60 µs (see Figs. 4 and 5). So, for a quantitative description of the measured pressure wave at later times a more sophisticated model including the pressure sensor was needed and developed.

The ASTE target consists of a cylindrical, 2.5 mm thick steel hull of 20 cm diameter with a hemispherical beam window and at the opposite side with a thick flange. Figure 3 shows the FEM model of a quarter of the ASTE target including the pressure sensor port close to the front end of the target.

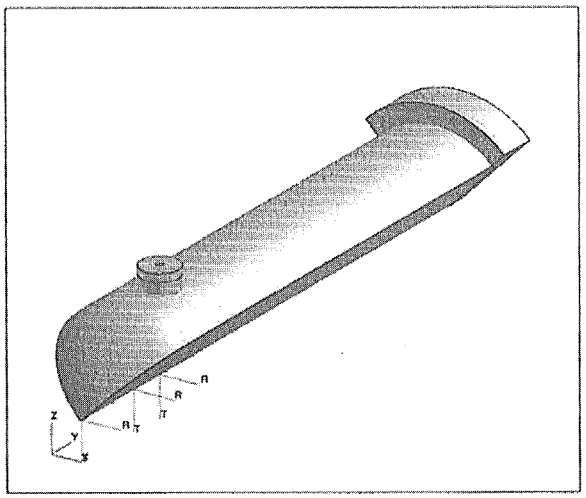

Fig. 3: The FEM model of a quarter of the ASTE mercury target

This port of 5 cm diameter is equipped with a mechanical pressure sensor, which is a thin (0.3 - 0.4 mm) circular steel membrane joined to a proper flange. Its displacements from the equilibrium position are measured with laser interferometry and converted into pressure values with the help of a static calibration of the sensor. The sensor was modeled and meshed and FEM static calculations were performed confirming the experimental calibration. Its eigen frequencies were calculated to identify them if accidentally excited.

In a first step a simplified FEM geometry on the ASTE target was modeled, in which the flange and pressure sensor were not taken into account. For different radii of the circular beam cross section and also for different deposited energies, the pressure values for times up to 400 μs after the proton pulse were calculated at the location in the mercury corresponding to the sensor position. One can see in Figs. 4 and 5 that the pressure is zero for the time the pressure wave front needs to travel at the velocity of sound (for mercury ca. 1400 m/s) from the zone in which it originated (corresponding to the beam profile contour) to the sampling zone.

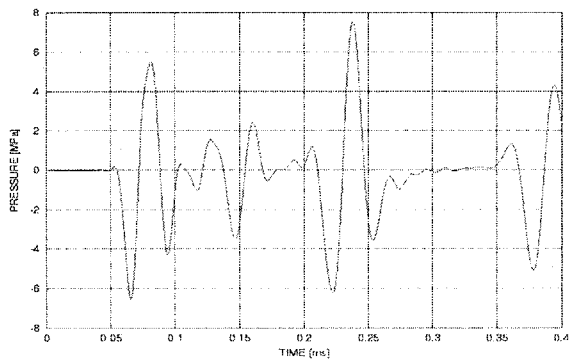

Fig. 4: Calculated time-dependent pressure in mercury at the location of the pressure sensor for a single pulse with a deposited energy of 10 kJ and a proton beam radius of 2 cm.

The bigger the beam radius (for given deposited energy) the smoother and smaller are the peaks where the mercury is under tensile stresses (positive values in Figs. 4 and 5). It seems worthwhile to point out that this fact may offer a means of mitigating the impact of pressure waves on the target structural materials.

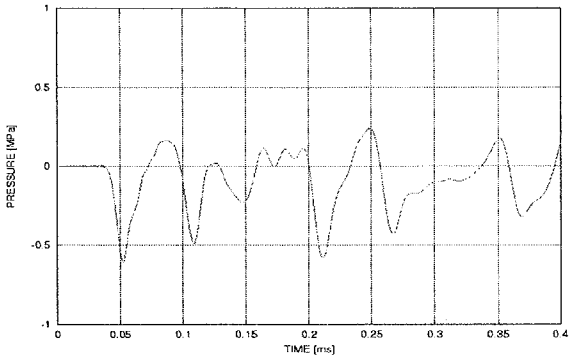

Fig. 5: Calculated time-dependent pressure in mercury at the location of the pressure sensor for a single pulse with a deposited energy of 10 kJ and a proton beam radius of 4 cm.

The agreement between calculations and experiment (not shown) is good only for the first 70 μs in which the value and the shape of the first peak in compression (negative values in Figs. 4 and 5) resembles the measured one. But, importantly, for later times the oscillations differ completely from experiment. A possible reason for this discrepancy may be the fact that the pressure has been calculated in the mercury at the location of the sensor, but not taking into account the dynamical behavior of the sensor itself. Therefore, a less simplified geometry including the sensor flange and the pressure sensor was modeled and meshed. A detail of the mesh for the measurement flange and the upper part of the sensor is shown in Fig. 6.

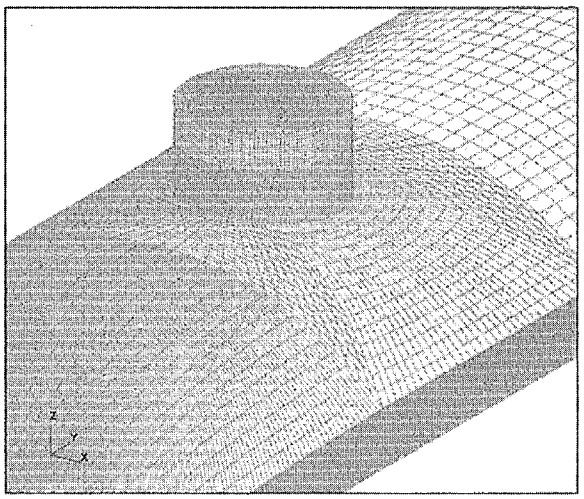

Fig. 6: Detail of the mesh used for modeling the pressure sensor location of one quarter of the ASTE target

4. Heat transfer experiments for target container proton beam windows

Strong thermo-mechanical loads are to be expected on the proton beam window of the mercury target container due to temperature gradients as well as transients due to accelerator tripping. Temperature gradients will arise due to the fact that the window is planned to be actively cooled only from the inner, the mercury side. Anyway, adequate cooling of the proton beam window is of utmost importance, even if it can be only done by the mercury itself. Therefore, extended test programs for investigating the heat transfer conditions have been devised [7]. Measurement techniques for determining transfer coefficients have been developed and experiments performed, which are compared to computational fluid dynamics

results. The experimental configuration has been designed according to the chosen concept of steering the mercury flow through the ESS target container as well as past the proton beam window as shown in Fig. 7.

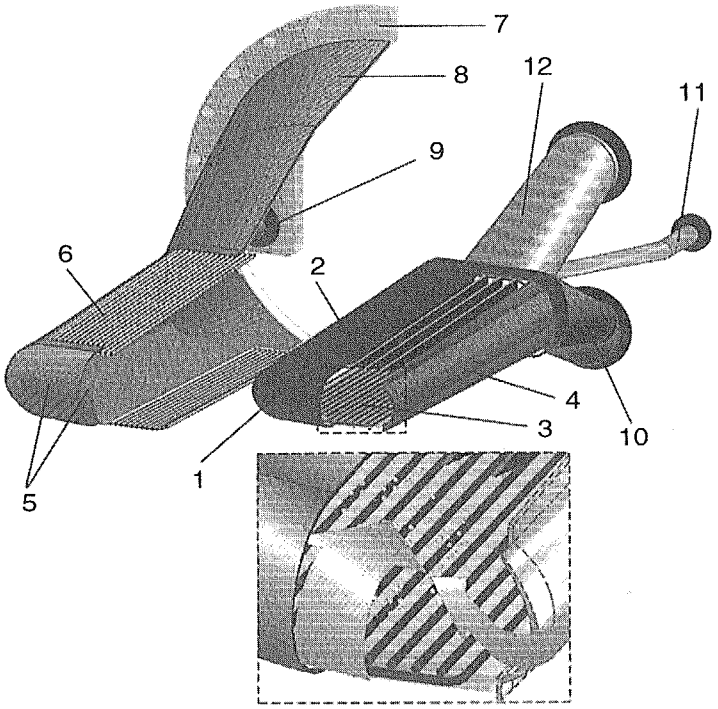

Fig. 7: Cutaway drawing of the ESS target container indicating the forced mercury flow past the proton beam window

For the heat transfer experiments a mercury loop and a target test section have been designed and installed at the Institute of Physics of the University of Latvia in Riga. The most essential part of the test section are the HETSS (Heat Emitting Temperature Sensing Surface) sensors, thin fiberglass-copper composite strips attached to the wall to be cooled by the mercury flowing past the sensors. Details on the HETSS sensors may be found elsewhere [8]. An exploded view of the test section is shown in Fig. 8 and an example of a comparison of experimental data with computational fluid dynamics results is shown in Fig. 9.

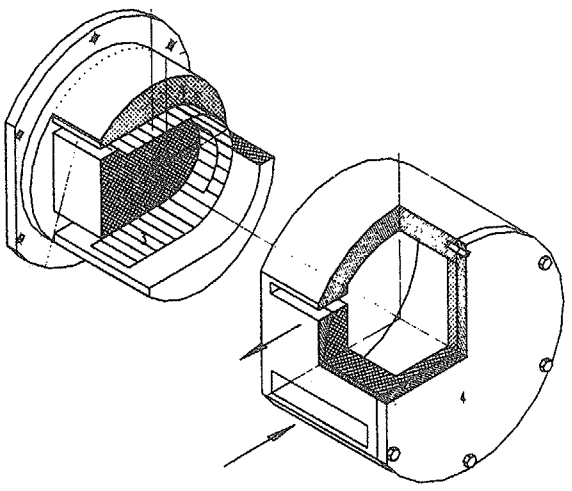

Fig. 8: Exploded view of the test section for heat transfer measurements. The HETSS sensor strip along the flow channel can be seen in the left. From [7].

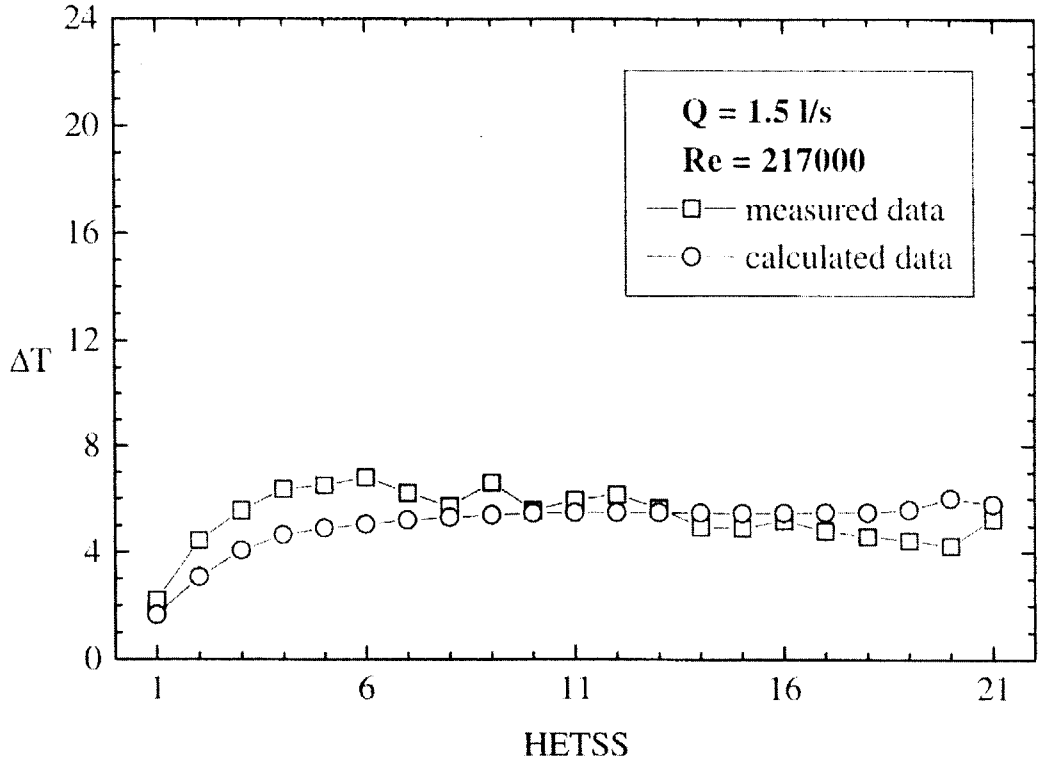

Fig. 9: Measured and calculated temperature differences for a particular flow rate and Reynold's number using HETSS sensors. From [7].

5. Advanced Cold Moderator development

Cold moderators have gained increasing importance in the past. Quality and quantity of neutrons produced with a pulsed source can be particularly improved, if cold moderators can deliver and sustain short pulses over a broad energy range. The ideal slowing down medium for that purpose is methane because of its high proton density and many low lying rotational vibration modes. But, as well known experience at IPNS and ISIS has shown, highly active radicals are formed in methane, in particular CH_3^- und H^+. In liquid methane (100-K-moderator) this gives rise to the formation of higher alkane homologues, which is eventually clogging the piping. In its solid state (20-K-moderator), in addition to radiolysis, crystal defects like interstitials are generated. The stored energy together with recombination of radicals can lead to spontaneous energy release (Wigner effect), which in turn may destroy the moderator vessels.

Within the present ESS R&D phase several paths for developing radiation resistant or at least better manageable cold moderators are being followed. One way is the production of small methane pebbles (2 to 3 mm diameter), which as a bed are cooled by flowing liquid hydrogen. A detailed account of the technological steps for producing methane pellets has been presented during the last ICANS meeting [9]. A second possibility is the inclusion of methane in porous substances (e.g. zeolites) or clathrates (e.g. from water ice), both again as small pebbles. Radiation damage and Wigner effect will thus be restricted to small particles. A timely and regular exchange of the pebble beds would prevent the destruction of the vessel and sustain the neutronic quality of the moderator. A third way would be the utilization of dif-

ferent hydrocarbons (with many freely rotating methyl groups), which do not exhibit the unfavorable radiolysis behavior of methane.

Irradiation behavior of pelletized moderator media are being performed at the pulsed reactor IBR-2 in Dubna. A detailed account of these irradiation experiments is given in an recent ESS report [10].

The neutronic properties (intensities and pulse shapes) of the different variants will be studied in a to scale mock-up of the ESS target-moderator-reflector module. The construction of this test facility at the cooler synchrotron (COSY) of Forschungszentrum Jülich had been finished recently and produced first results [11]. These experiments are performed under the auspices of the international collaboration JESSICA (Jülich Experimental Spallation target Set-up In COSY Area).

6. The ESS target/moderator/reflector mockup JESSICA

The JÜLICH EXPERIMENTAL SPALLATION TARGET SET-UP IN COSY AREA (JESSICA) is a to scale mock-up of the ESS target/moderator/reflector assembly. A detailed presentation of its design and experimental goals is given in a separate paper [11]. The main purpose of JESSICA is the optimization of the target and moderator efficiency, in particular with respect to the neutronics of advanced cold moderators. The JESSICA experimental hall is shown in Fig. 11.

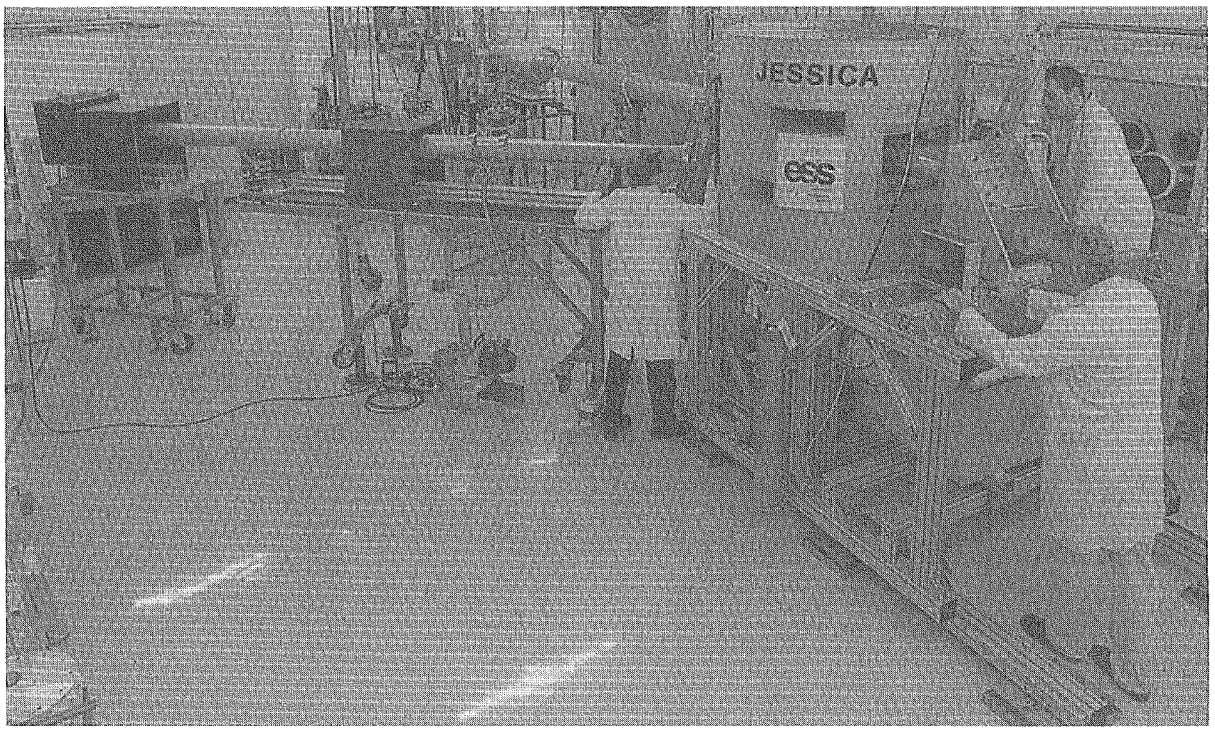

Fig. 10: JESSICA room at COSY (FZ Jülich). The proton beam line can be seen at top center, the neutron flight path from target-moderator-reflector module to the left (shielding partly removed).

References

[1] H. Ullmaier and F. Carsughi, Nucl. Instr. Methods B101 (1995) 406
[2] F. Carsughi, these Proceedings
[3] F. Carsughi, H. Derz, P. Ferguson, G. Pott, W.F. Sommer and H. Ullmaier, J. Nucl. Mater. 264 (1999) 78
[4] Y. Dai, G. Bauer, F. Carsughi, H. Ullmaier, S.A. Malloy and W.F. Sommer, J. Nucl. Mater. 265 (1999) 203
[5] J. Chen, Y. Dai, F. Carsughi, W.F. Sommer, G.S. Bauer and H. Ullmaier, J. Nucl. Mater. 275 (1989) 115
[6] Liping Ni, ESS 97-65-T (1997)
[7] I. Bucenieks et al.; ESS 98-73-T (1998)
[8] I. Platnieks et al.; Proceedings ICANS-XIV (1998)
[9] H. Barnert-Wiemer, Proceedings ICANS-XIV (1998)
[10] E.P. Shabalin et al., ESS 99-92-T (1999), ISSN1433-559X
[11] H. Tietze-Jaensch et al., these Proceedings